Pumped hydroelectric storage balances a solar microgrid

Hydro Research Foundation report

Kevin J. Kircher, Cornell University
Faculty Adviser: K. Max Zhang

Abstract

We consider the problem of reliably operating a microgrid with solar generation and pumped hydroelectric storage. We show that reliable operation is possible if storage equipment is sufficiently flexible and storage control is sufficiently robust to solar variability. Pumped storage flexibility can be achieved through a ternary configuration; this enables rapid switching between pumping and generating modes. Controller robustness can be achieved through a novel control synthesis method based on convex optimization and resampled historical solar data. The proposed equipment and controller perform well in simulations including twenty months of real solar data at five minute resolution. These results highlight the potential of pumped storage to enable reliable integration of wind and solar power into the grid.

1 Introduction

In many regions and applications, wind and solar power are now economically attractive. However, wind and solar power are variable and uncertain. This complicates grid operators' task of continually balancing electricity supply and demand. More flexibility is needed to reliably integrate random renewables. This need is especially pronounced in microgrids, which have low inertia and little spatial resource diversity. In this project, we investigate the potential of pumped storage to balance renewable microgrids. We approach this question through a challenging case study.

1.1 Case study

The state of Hawai'i imports 85% of its food. Imported fossil fuels supply 90% of its energy. Hawai'ian electricity is the most expensive in the U.S., costing about 42 ¢/kWh. Meanwhile, Hawai'i has excellent resources for agriculture and renewable energy. These facts make local, sustainable food and energy projects in Hawai'i economically and environmentally attractive.

Hydropower is particularly attractive in Hawai'i due to the state's extensive irrigation infrastructure. This infrastructure once supported sugar plantations, but has been underutilized since the sugar industry collapsed in the 1990s. In some areas, the state's revenues from water use are insufficient to fund needed infrastructure maintenance. This jeopardizes marginalized communities in remote areas that depend on irrigation infrastructure. Revitalizing irrigation infrastructure for hydropower could increase state revenues, funding needing maintenance while providing sustainable energy.

In this project, we study the case of a sustainable farming community on the Big Island of Hawai'i. Our collaborators, a group of native Hawai'ian farmers, are interested in building a shared commercial kitchen. The proposed location is close to farms but far from the electricity distribution network. For this reason, our collaborators are interested in the technical feasibility of powering the kitchen via a microgrid. Renewable generation is preferred.

The location has ample sunshine, steep hills and unused reservoirs at several elevations. There is an irrigation ditch nearby, but water withdrawals are prohibitively expensive for direct hydropower generation. We propose solar photovoltaics as the primary energy source. In [1], Ma *et al.* showed that in islanded microgrids, lifetime costs of pumped storage are lower than batteries by a factor of two to three. Our site-specific economic analysis supports this conclusion (see the supporting documents *Hydropower on the Lower Hamakua Ditch* and *Microgrid Farming Communities in Hawai'i* for more discussion). Therefore, we propose pumped storage for grid balancing.

1.2 Microgrid components

Supply. Electricity supply comes from a solar photovoltaic array sized to meet energy demand after adjusting for storage losses. We simulate the array power output by resampling historical data provided by a Hawai'ian collaborator at a nearby facility. The data include the power output from five solar arrays over four months at five minute resolution.

Demand. Electricity demand comes from cooling and ventilating the commercial kitchen and powering its refrigerators and other appliances. We simulate this demand using the Matlab `bldg` toolbox, a nonlinear testbed that includes the random effects of weather and occupant behavior. [2] Demand is about 14 kW on average and 22 kW at peak.

Storage. We consider ternary pumped storage: upper and lower reservoirs, a hydraulic bypass, and a Pelton impulse turbine suitable for our high-head, low-flow application. Figure 1 illustrates the system. The ternary configuration enables simultaneous pumping and generation. This has mathematical properties that facilitate control. It also enables transition times between pure-pumping and pure-generation modes on the order of thirty seconds, compared to the several minutes required for transitions in reversible-flow systems. [3, 4] This has advantages in our solar microgrid, where generation can fluctuate rapidly due to fast-moving clouds.

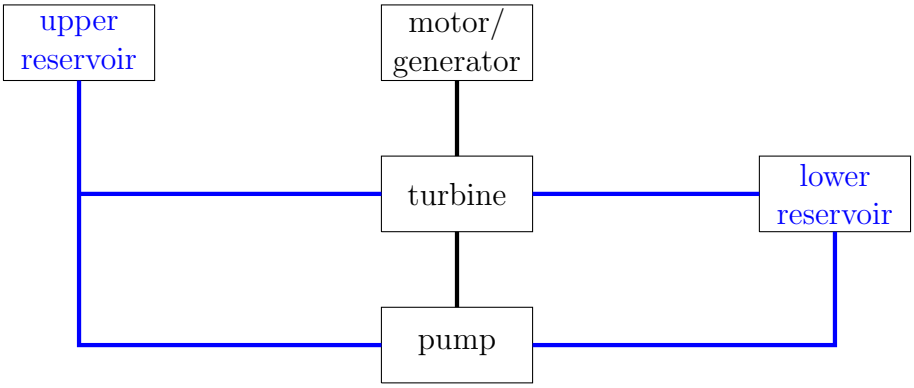

Figure 1: A ternary pumped storage system. Blue lines represent water flow. A single shaft (black) connects the motor/generator, turbine, and pump. This setup enables rapid switching between pumping and generating.

2 Microgrid control

Following the control hierarchy described in [5], we restrict our attention to secondary control (time steps on the order of minutes). We assume that primary control (time steps of seconds or faster) is provided by a fast feedback controller. Primary actuation could come from variable speed drives on the pumped storage machinery or from a small battery, capacitor or flywheel.

The secondary storage control problem is to decide the uphill and downhill water flows in order to robustly maintain the power and energy imbalances within the capacities of the primary balancing equipment. The secondary controller must also respect capacity constraints on the volume of water stored and the flow rates through the pump and generator.

2.1 Dynamics

We assume that the pumped storage is a closed system, so the total volume of water is conserved. The storage state can therefore be characterized by x_1 (m^3), the volume of water in the upper reservoir. In terms of the uphill and downhill water flows u_1 and u_2 (m^3/s), the storage dynamics are

$$x_1(t+1) = x_1(t) + \Delta t(u_1(t) - u_2(t)), \quad t = 0, \ldots, T-1. \tag{1}$$

Here t indexes discrete time with time step Δt and horizon T. We assume perfect state information is available.

We seek to balance the power supply

$$s(t) = \eta_g \rho g h u_2(t)$$

and demand

$$d(t) = w(t) + \rho g h u_1(t)/\eta_p,$$

both instantaneously and on average. To do so, we keep track of the instantaneous shortfall

$$y(t) = d(t) - s(t)$$

and the cumulative shortfall x_2 (kWh). The cumulative shortfall dynamics are

$$x_2(t+1) = x_2(t) + \Delta t y(t), \quad t = 0, \ldots, T-1. \tag{2}$$

In the equations above, $\rho = 1000$ kg/m^3 is the density of water, $g = 9.8$ m/s^2 is the acceleration of gravity, h (km) is the height from the lower to upper reservoir and w (kW) is the net load, *i.e.*, the load minus solar generation. We assume that the pump and generator efficiencies, $\eta_p, \eta_g \in (0, 1]$, are approximately constant.

The dynamics (1) and (2) can be written compactly as

$$x = Ax(0) + Bu + Cw.$$

Here A, B and C are suitably defined matrices. The state, control and disturbance trajectories are

$$\begin{aligned} x &= (x(1), \ldots, x(T)) \\ u &= (u(0), \ldots, u(T-1)) \\ w &= (w(0), \ldots, w(T-1)). \end{aligned}$$

2.2 Constraints

The storage system has volume, pumping and generation constraints:

$$\begin{aligned} 0 \leq x_1(t) \leq \bar{x}_1, &\quad t = 1, \ldots, T \\ 0 \leq u_1(t) \leq \bar{u}_1, &\quad t = 0, \ldots, T-1 \\ 0 \leq u_2(t) \leq \bar{u}_2, &\quad t = 0, \ldots, T-1. \end{aligned}$$

Here $\bar{x}_1$ (m^3) is the upper reservoir volume and $\bar{u}_1$ and $\bar{u}_2$ (m^3/s) are the uphill and downhill flow limits. These constraints can be written as

$$g(u) \preceq 0,$$

where $g : \mathbf{R}^{2T} \to \mathbf{R}^{6T}$ is defined by

$$g(u) = \begin{bmatrix} -\left(I \otimes \begin{bmatrix} 1 & 0 \end{bmatrix}\right)(Ax(0) + Bu) \\ \left(I \otimes \begin{bmatrix} 1 & 0 \end{bmatrix}\right)(Ax(0) + Bu) - \bar{x}_1 \mathbf{1} \\ -u \\ u - \mathbf{1} \otimes \begin{bmatrix} \bar{u}_1 \\ \bar{u}_2 \end{bmatrix} \end{bmatrix}.$$

In the above, I is an identity matrix, $\mathbf{1}$ is a vector of ones and $\otimes$ denotes the Kronecker product.

Many storage systems, such as batteries or non-ternary pumped storage, prohibit simultaneous charging and discharging. This gives rise to a constraint of the form

$$u_1(t)u_2(t) = 0.$$

This nonlinear equality constraint is nonconvex. Imposing it greatly complicates optimization, requiring different algorithms and making guarantees of global optimality unavailable. The ternary pumped storage configuration eliminates these complications by allowing simultaneous charging and discharging.

2.3 Cost

As we are interested in limiting the required power and energy capacities of the primary balancing equipment, we penalize a weighted sum of the maximum instantaneous and cumulative imbalances over the control horizon,

$$\|y\|_\infty + \gamma \|x_2\|_\infty .$$

Here $y = (y(1), \ldots, y(T))$ is the instantaneous shortfall trajectory and $x_2 = (x_2(1), \ldots, x_2(T))$ is the cumulative shortfall trajectory. The tunable parameter γ governs the tradeoff between the power and energy shortfalls. It has units of inverse hours. It can be interpreted as the ratio of a \$/kWh energy price to a \$/kW power price. In terms of the control and disturbance trajectories, the cost can be written as

$$\begin{aligned} f(u, w) = &\left\| w + \rho g h \left(I \otimes \begin{bmatrix} 1/\eta_p & -\eta_g \end{bmatrix} \right) u \right\|_\infty \\ &+ \gamma \left\| \left(I \otimes \begin{bmatrix} 0 & 1 \end{bmatrix} \right) (Ax(0) + Bu + Cw) \right\|_\infty . \end{aligned}$$

2.4 Risk measure

The cost $f(u, w)$ depends on the disturbance w. Similarly, when the control is decided based on feedback, the constraint $g(u)$ depends implicitly on w through u. The goals of minimizing $f(u, w)$ and constraining $g(u)$ are therefore ambiguous: do we wish to accomplish them for a particular realization of w, in expectation with respect to the distribution of w, for all possible w, or something else? Answering this question amounts to deciding how to measure risk; see [6] for details.

We choose to measure risk by the worst-case value over all possible net load trajectories. This is a coherent measure of risk in the sense of [7]. We investigated other risk measures, such as the expected value and conditional value at risk [8, 9], but found that the worst-case value gave the best performance for this problem.

2.5 Problem statement

In the general framework of control under uncertainty, the optimization is over causal state feedback policies $\pi = (\pi_0, \ldots, \pi_{T-1})$ such that

$$u = \pi(x) = \begin{bmatrix} \pi_0(x(0)) \\ \pi_1(x(0), x(1)) \\ \vdots \\ \pi_{T-1}(x(0), x(1), \ldots, x(T-1)) \end{bmatrix}.$$

The control problem, therefore, is to

$$\begin{array}{ll} \underset{\pi}{\text{minimize}} & \max_w f(u, w) \\ \text{subject to} & \max_w g(u) \preceq 0 \\ & x = Ax(0) + Bu + Cw \\ & u = \pi(x). \end{array} \tag{3}$$

2.6 Approximate solution

Problem 3 is intractable for three reasons. First, it is nonconvex due to the dependence of u on x and x on u. Second, the feasible region (the space of all causal state feedback policies) is infinite-dimensional. Third, the distribution of the net load w is unknown. To arrive at a tractable problem, we use two approximations: (1) optimizing over finite-dimensional, affine disturbance feedback policies, and (2) relaxing the risk measure to the worst-case value over N randomly sampled net load trajectories.

2.6.1 Policy parameterization

Because state feedback policies are vector-valued functions, stochastic control problems are infinite-dimensional in general. To arrive at a finite-dimensional problem, we reparameterize the control law as affine state feedback,

$$u = v + Kx.$$

Causality implies that the matrix K is strictly block lower triangular.

This parameterization results in a nonconvex optimization problem. Convexity can be achieved by reparameterizing the control law as affine disturbance feedback, as in [10]:

$$u = q + \tilde{Q}w.$$

The affine state and disturbance feedback policies are equivalent in the following sense. Recalling that $x = Ax(0) + Bu + Cw$, and assuming that $I - KB$ is nonsingular, we have

$$\begin{aligned} u = v + Kx &= v + K(Ax(0) + Bu + Cw) \\ \implies \quad u &= (I - KB)^{-1}(v + K(Ax(0) + Cw)) \\ &= (I - KB)^{-1}(v + KAx(0)) + (I - KB)^{-1}Cw \\ &= q + \tilde{Q}w. \end{aligned}$$

This is related to the Q or Youla parameterization; see [11] for discussion.

Optimizing over the matrix $\tilde{Q} \in \mathbf{R}^{2T \times T}$ introduces $2T^2$ decision variables. To reduce the dimension of the resulting optimization problem, we further restrict the search space to policies with a memory of a single time step, so that

$$\begin{aligned} u(0) &= q(0) \\ u(t) &= q(t) + Qw(t-1), \quad t = 1, \ldots, T-1. \end{aligned} \tag{4}$$

We investigated affine policies with longer memory, but found that they did not improve performance much over the one-stage policy.

With this parameterization, we arrive at an approximate problem:

$$\begin{array}{ll} \underset{q,Q}{\text{minimize}} & \max_w f(u, w) \\ \text{subject to} & \max_w g(u) \preceq 0 \\ & u(0) = q(0) \\ & u(t) = q(t) + Qw(t-1), \quad t = 1, \ldots, T-1. \end{array} \tag{5}$$

2.6.2 Sampling

Because the distribution of the net load w is unknown, the maxima in problem (5) cannot be computed. We approximate them by generating sample disturbance trajectories $w^1, \ldots, w^N$ from the distribution of w, then solving the following problem:

$$\begin{array}{ll} \underset{q,Q}{\text{minimize}} & \max\left\{f(u^1, w^1), \ldots, f(u^N, w^N)\right\} \\ \text{subject to} & g(u^i) \preceq 0, \quad i = 1, \ldots, N \\ & u^i(0) = q(0), \quad i = 1, \ldots, N \\ & u^i(t) = q(t) + Qw^i(t-1), \quad t = 1, \ldots, T-1, \quad i = 1, \ldots, N. \end{array} \tag{6}$$

This approach is related to sample-average approximation (see [11–14]) and other scenario approximations for optimization under uncertainty (see [15–17]).

2.7 Complexity

Because g and $f(\cdot, w)$ are convex functions and the pointwise maximum preserves convexity, problem (6) is an instance of convex programming. The $2(T+1)$ decision variables are the elements of $q \in \mathbf{R}^{2T}$ and $Q \in \mathbf{R}^2$. The equality constraints can be straightforwardly eliminated, leaving $6NT$ inequality constraints. Although this is a large-scale problem, it can be solved to global optimality in polynomial time using, *e.g.*, interior-point methods. Such methods typically require a few tens of iterations to converge to a solution. The main work in each iteration is evaluating the objective and constraint functions and their first and second derivatives; this takes on the order of NT^3 operations. The cubic dependence on T makes long-horizon problems challenging to solve; this suggests that a model predictive control strategy with a truncated horizon might be effective. We note, however, that problem (6) can be solved for q and Q offline. No online optimization is necessary. Online evaluation of the policy (4) is extremely efficient.

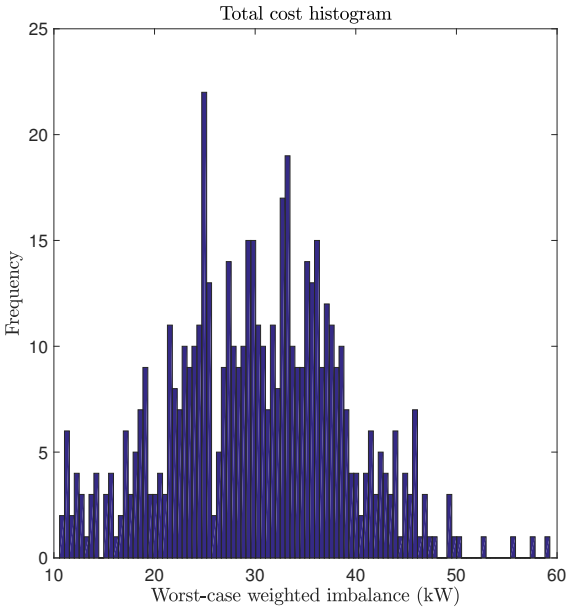

Figure 2: Histogram of the total cost, a weighted sum of the worst-case power and energy imbalances, over 550 one-day Monte Carlo simulations with five minute time steps. The worst imbalances were about 20 kW and 10 kWh.

3 Simulation

We simulated controller performance over each of the $M = 550$ days in the historical solar dataset. We used a time step of $\Delta t = 5$ minutes, giving a horizon of $T = 288$. We investigated the sensitivity of controller performance to the number of training samples. We found that $N = 20$ gave a good trade-off between optimization time and controller performance. Similarly, we found that a value of $\gamma = 1/\Delta t$ gave a good trade-off between power and energy balancing. Optimization modeling was done in the Matlab CVX toolbox [18]. Optimization problems were solved in SDPT3. [19]

The physical parameters in the simulations are $h = 40$ m, 90% efficiencies for the pump and generator, reservoir volumes of about 3.5 thousand m^3 (about 375 kWh of energy storage), and pump and generator flow capacities of 0.14 m^3/s (about 60 kW). These capacities were chosen in an ad hoc way; we expect that the storage, pump and generator could be downsized significantly with no impact on performance. In all Monte Carlo runs, an initial storage state of 50% was used.

Figure 2 shows a total cost histogram over all the Monte Carlo runs. The worst-case power imbalance, over all 550 net load scenarios, was about 20 kW. The worst-case energy imbalance was about 10 kWh. This suggests that relatively small primary balancing equipment is sufficient.

Figures 3 and 4 show the water and power trajectories over a typical Monte Carlo run. Balancing is essentially perfect when the sun is down; the controller is easily able to balance

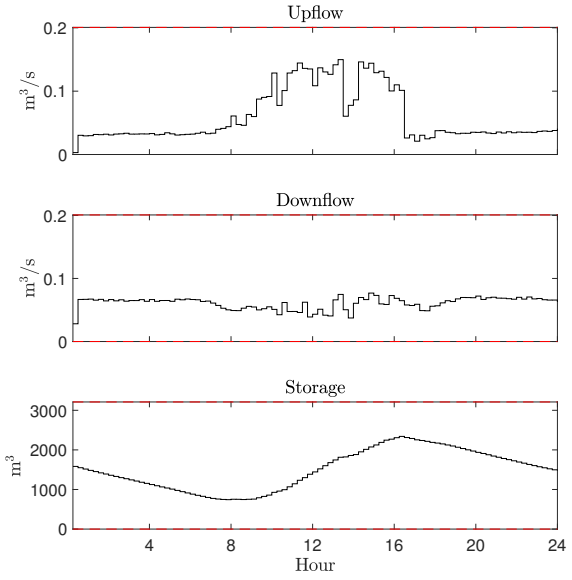

Figure 3: Water trajectories in a typical Monte Carlo run. The controller uses the simultaneous pumping and generating ability of the ternary storage system to help balance net load fluctuations. Flow and volume constraints are easily respected, suggesting that the system could be significantly downsized.

the relatively small fluctuations in load. However, when the sun is up on this partly cloudy day, cloud motion makes the solar power output highly volatile. The secondary controller can balance some, but not all, of these solar fluctuations. The remaining balancing must be performed at the primary control level by, for example, feedback control of variable speed pumped storage equipment.

4 Conclusion

In this project, we explored secondary control of a microgrid with solar photovoltaic generation and pumped storage. We formulated a robust optimal control problem and used two approximations to enable tractable, if suboptimal, control synthesis. The resulting controller has an affine disturbance feedback form. It respects hard equipment constraints and minimizes the worst-case power and energy imbalances. The controller was validated through Monte Carlo simulation over 550 days of real solar data with five minute resolution.

The practical impact of this work is to demonstrate that pumped storage can balance the variability of solar power. On the hardware side, this is enabled by the highly flexible and controllable ternary pumped storage configuration. The ternary configuration enables rapid switching between pumping and generating modes in order to balance solar fluctuations. In our application, the estimated lifetime cost of pumped storage is lower than that of batteries by a factor of two to three. On the software side, reliable operation is enabled by paying

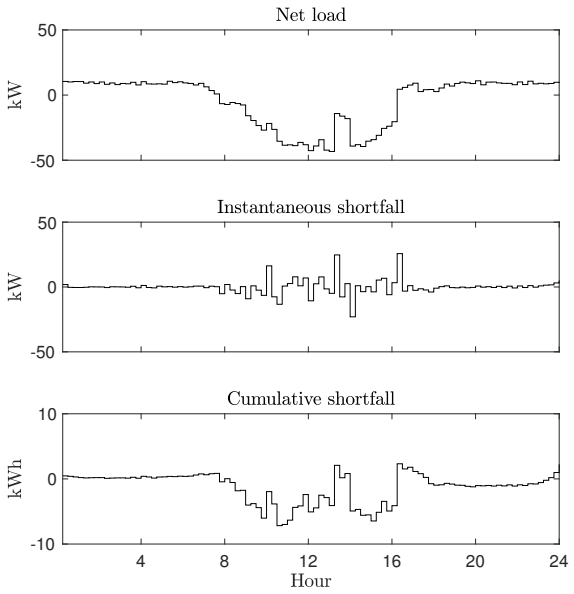

Figure 4: Power trajectories in the Monte Carlo run in Figure 3. The power imbalance is largest when the net load is most volatile due to large, rapid solar fluctuations.

careful attention to the uncertainty and volatility of solar power. The control design method we proposed, which uses convex optimization and resampled historical data, has applications beyond this problem.

There are a number of opportunities to extend this work. First, primary microgrid control (time steps of seconds or faster) via variable speed pumped hydroelectric equipment could be investigated. Second, the robust affine disturbance feedback policy used here for secondary control could be compared to nonlinear control strategies such as model predictive control. Third, the problem of combined equipment sizing and control synthesis could be investigated.

5 Acknowledgments

The authors are grateful to the Hydro Research Foundation for funding this work and for providing extensive technical and practical insights. We are particularly thankful for the assistance of Brenna Vaughn, who could not have been kinder or more patient.

References

1. Ma, T., Yang, H. & Lu, L. Feasibility study and economic analysis of pumped hydro storage and battery storage for a renewable energy powered island. *Energy Conversion and Management* **79,** 387–397 (2014).

2. Kircher, K. J. & Zhang, K. M. *Testing building controls with the BLDG toolbox* in *American Control Conference (ACC)* (2016).
3. Koritarov, V. *et al. Modeling Ternary Pumped Storage Units* tech. rep. ANL/DIS-13/07 (Argonne National Laboratory, 2013).
4. Botterud, A., Levin, T. & Koritarov, V. *Pumped storage hydropower: benefits for grid reliability and integration of variable renewable energy* tech. rep. ANL/DIS-14/10 (Argonne National Laboratory, 2014).
5. Olivares, D. *et al.* Trends in microgrid control. *Smart Grid, IEEE Transactions on* **5,** 1905–1919 (2014).
6. Rockafellar, R. T. Coherent approaches to risk in optimization under uncertainty. *OR Tools and Applications: Glimpses of Future Technologies.* 38–61 (2007).
7. Artzner, P., Delbaen, F., Eber, J. M. & Heath, D. Coherent measures of risk. *Mathematical Finance* **9,** 203–288 (1999).
8. Rockafellar, R. T. & Uryasev, S. Optimization of conditional value-at-risk. *Journal of risk* **2,** 21–42. (2000).
9. Rockafellar, R. T. & Uryasev, S. Conditional value-at-risk for general loss distributions. *Journal of Banking and Finance* **26,** 1443–1471 (2002).
10. Oldewurtel, F., Jones, C. & Morari, M. *A tractable approximation of chance constrained stochastic MPC based on affine disturbance feedback* in *Conference on Decision and Control* (2008).
11. Skaf, J. & Boyd, S. Nonlinear Q-design for convex stochastic control. *IEEE Transactions on Automatic Control* **54,** 2426–2430 (2009).
12. Homem-de-Mello, T. & Bayraksan, G. Monte Carlo sampling-based methods for stochastic optimization. *Surveys in Operations Research and Management Science* **19,** 56–85 (2014).
13. Kim, S., Pasupathy, R. & Henderson, S. G. *A guide to sample average approximation* in *Handbook of Simulation Optimization* (Springer New York, 2015), 207–243.
14. Kircher, K. J. & Zhang, K. M. *Sample-average model predictive control of uncertain linear systems* in *Conference on Decision and Control* (2016), 6234–6239.
15. Calafiore, G. & Campi, M. Uncertain convex programs: Randomized solutions and confidence levels. *Mathematical Programming* **102,** 25–46 (2005).
16. Campi, M. & Garatti, S. The exact feasibility of randomized solutions of uncertain convex programs. *SIAM Journal on Optimization* **19,** 1211–1230 (2008).
17. Calafiore, G. Random convex programs. *SIAM Journal on Optimization* **20,** 3427–3464 (2010).
18. Grant, M. & Boyd, S. *CVX: Matlab Software for Disciplined Convex Programming, version 2.0 beta* Sept. 2013. http://cvxr.com/cvx.

19. Toh, K., Todd, M. & Tutuncu, R. SDPT3 – a Matlab Software Package for Semidefinite Programming. *Optimization Methods and Software* **11,** 545–581 (1999).